ISSN 0030-400X, Optics and Spectroscopy, 2012, Vol. 113, No. 1, pp. 23–32. © Pleiades Publishing, Ltd., 2012.

SPECTROSCOPY OF ATOMS AND MOLECULES

DFT Simulations, FT-IR, FT-Raman, and FT-NMR Spectra of 4-(4-Chlorophenyl)-1H-imidazole Molecules[1]

Y. Erdogdu[a], M. T. Güllüoğlu[a], Ş. Yurdakul[b], and Ö. Dereli[c]

[a] *Department of Physics, Ahi Evran University, 40040 Kirsehir, Turkey*

[b] *Department of Physics, Gazi University, 06500 Ankara, Turkey*

[c] *A. Kelešoğlu Education Faculty, Department of Physics, Selcuk University, 42090 Konya, Turkey*

Received November 24, 2011

Abstract—The FT-IR, FT-Raman and FT-NMR spectra of the compound 4-(4-Chlorophenyl)-1H-imidazole (4-ClPI) was recorded and analyzed. Density functional method has been used to compute optimized geometry, vibrational wavenumbers and NMR spectra of the 4-ClPI. Only one tautomeric form was found most stable by using B3LYP functional with the 6-311++G(*d*,*p*) as basis sets. The detailed interpretation of the vibrational spectra was carried out with the aid of total energy distribution (TED) following the scaled quantum mechanical force field methodology.

DOI: 10.1134/S0030400X12070089

INTRODUCTION

Imidazole is nitrogen containing heterocyclic ring which possesses biological, pharmaceutical and unique optical properties. Thus, imidazole compounds have been an interesting source for researchers for more than a century [1, 2]. Heterocyclic imidazole derivatives plays very important role in chemistry as mediators for synthetic reactions, primarily for preparing functionalized materials [2]. In addition, they are widely used in many fields, such as P38 MAP kinase [3], antivascular disrupting, antitumour activator [4], ionic liquids [5], anion sensors [2], as well as electrical and optical materials [6–8].

Imidazole derivatives show unique chemical and physical properties because they contain imidazole heterocycle which has better thermal stability, and benzene rings can increase the degree of conjugation of the organic molecule. Imidazole derivatives has also significant analytical applications by utilizing their fluorescence and chemiluminescence properties [9]. An important property that makes imidazole derivatives more attractive as a chelator is the appreciable change in its fluorescence upon metal binding. As a result, luminescent, materials of imidazole derivative have emerged as the attractive blue-emitting materials. Therefore, imidazole derivatives have been used to construct highly sensitive fluorescent chemisensors for sensing and imaging of metal ions and its chelates in particular those with Ir^{3+} are major components for organic light emitting diodes [9, 10] and are promising candidates for fluorescent chemisensors for metal ions. Recently the research by Huang and Zhao [11] was aimed at the production of imidazole derivatives for luminophores, but such materials are oligomers which restricted the application.

Organic luminescent materials have recently received much attention due to their potential applications in organic lightemitting diodes [12], ceramics [13], fluorescent biological labels [14], photovoltaic cells [15], and optical sensors [16]. A great number of luminescent organic materials have been synthesized and investigated, for example, recently the better blue lightemitting materials were achieved for the pyrazoloquinolihe chromophore, where the quantum efficiency was about 1.7 [17, 18]. However, organic luminescent materials still have stability problems and the correlation between structure and fluorescence efficiency remains a big challenge in this area.

FT-IR, FT-Raman and FT-NMR spectra of 4-phenylimidazole molecule using theoretical and experimental methods has been reported earlier [19]. In the present paper we deal with the IR, Raman and NMR spectra of 4-(4-Chlorophenyl)-1H-imidazole (4-ClPI) molecule along with the theoretical prediction using DFT method.

EXPERIMENTAL

The FT-IR spectrum of this molecule recorded in the region 4000–400 cm^{-1} on IFS 66V spectrophotometer using KBr pellet technique is shown in Fig. 1. The FT-Raman spectrum of 4-ClPI recorded using 1064 nm line of Nd : YAG laser as excitation wavelength in the region 50–3500 cm^{-1} on a Thermo Electron Corporation model Nexus 670 spectrophotometer equipped with FT-Raman module accessory are shown in Fig. 2. The ^{1}H and ^{13}C NMR spectra are taken in chloroform solutions and all signals are refer-

[1] The article is published in the original.

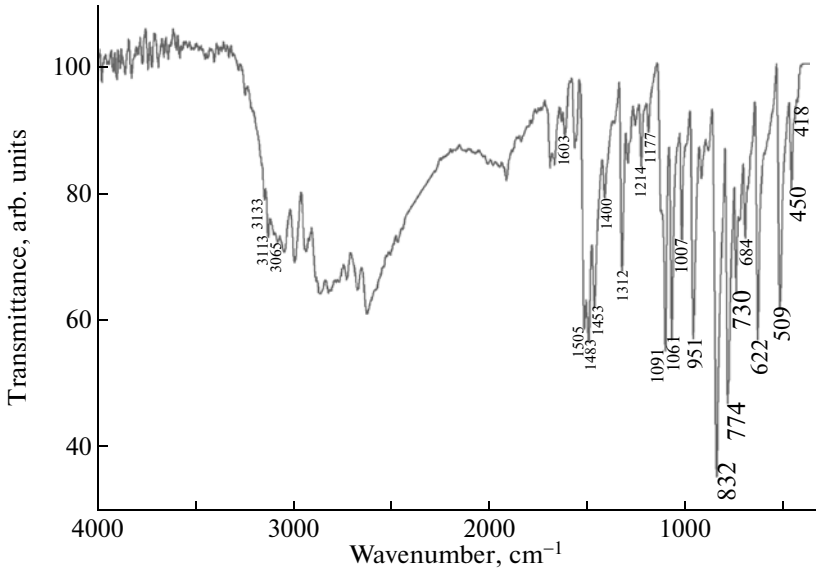

Fig. 1. FT-IR spectra of 4-ClPI molecule in the range 400–4000 cm^{-1}.

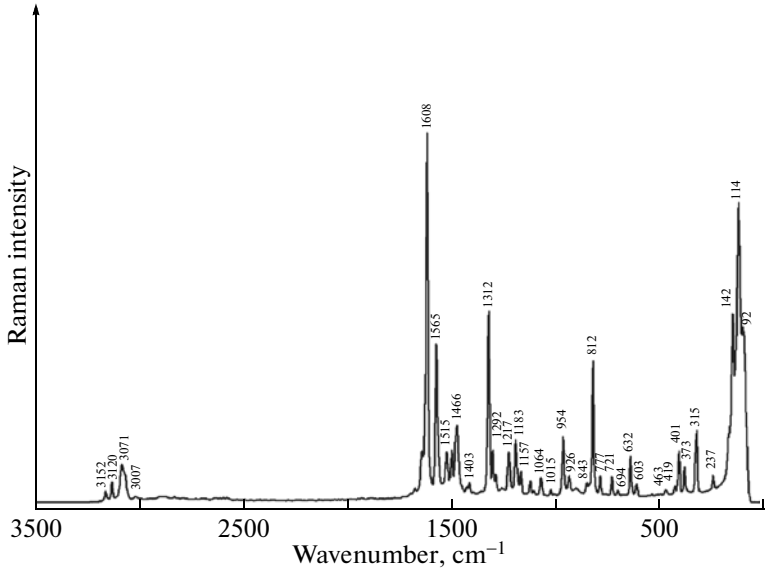

Fig. 2. FT-Raman spectra of 4-ClPI in the range 50–3500 cm^{-1}.

enced to TMS on a BRUKER DPX-400 FT-NMR Spectrometer All NMR spectra are measured at room temperature.

COMPUTATIONAL DETAILS

Gaussian 09 quantum chemical software was used in all calculations [20]. The optimized structural parameters and vibrational wavenumbers for the 4-ClPI molecule were calculated by using B3LYP functional with 6-311G++(*d*,*p*) as basis set. The vibrational modes were assigned on the basis of TED analysis using SQM program [21]. Normal coordinate analysis of the title molecules has been carried out to obtain a more complete description of the molecular motions involved in the fundamentals. The calculated harmonic vibrational wavenumbers were scaled down uniformly by a factor of 0.967 (for wave numbers under 1800 cm^{-1}) and 0.955 (for those over 1800 cm^{-1}) for B3LYP/6-311++G(*d*,*p*) level of theory, which accounts for systematic errors caused by basis set incompleteness, neglect of electron correlation and vibrational anharmonicity [22–24].

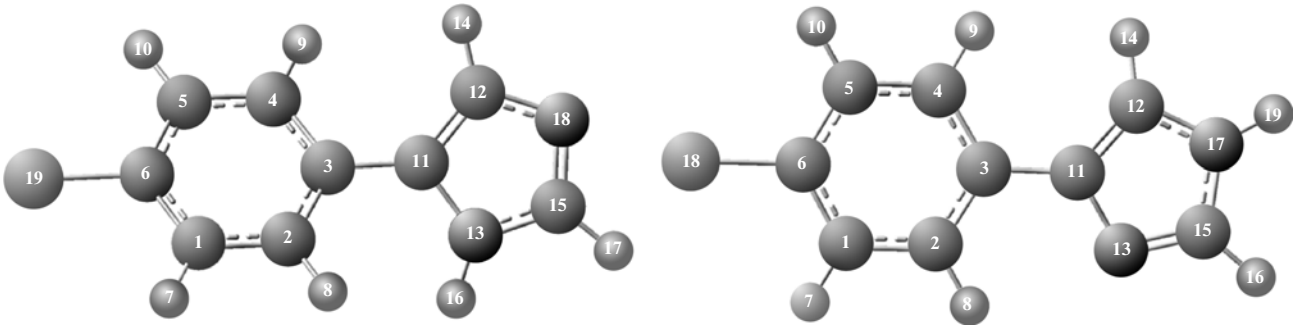

Fig. 3. Tautomeric forms and atomic numbers of 4ClPI.

The ^{1}H and ^{13}C NMR chemical shifts calculations of the T_2 tautomeric form of the 4-ClPI molecule were made by using B3LYP functional with 6-311G++(*d*,*p*) basis set. The GIAO (gauge including atomic orbital) method is one of the most common approaches for calculating isotropic nuclear magnetic shielding tensors [25, 26]. For the same basis set size GIAO method is often more accurate than those calculated with other approaches [27, 28]. The NMR spectra calculations were performed by Gaussian 09 program package. The calculations reported were performed in chloroform solution using IEF-PCM model as well as gas phase in agreement with experimental chemical shifts obtained in chloroform solution.

Predictions of Raman Intensities

It should be noted that Gaussian 09 package able to calculate the Raman activity. The Raman activities were transformed into Raman intensities using Raint program [29] by the expression

$$I_i = 10^{-12}(\nu_0 - \nu_i)^4 RA_i/\nu_i,$$

where I_i is the Raman intensity, RA_i is the Raman scattering activities, ν_i is the wavenumber of the normal modes, and ν_0 denotes the wavenumber of the excitation laser [30].

RESULTS AND DISCUSSION

Tautomeric Analysis

All the possible tautomeric forms of 4-ClPI were calculated which are optimized by B3LYP/6-311++G(*d*,*p*) level of theory. The possible two stable tautomeric forms are given in Fig. 3 which shows the possibility of proton transfer between the nitrogen atoms of imidazole ring. The total energies and the relative energies of the different tautomeric forms of 4-ClPI are presented in Fig. 3. Many attempts to investigate the tautomeric equilibrium structure of this molecule have been made using different calculation methods. It is determined that T_2 is more stable than T_1 by 3 kJ/mol for AM1 and PM3 calculations by Ogretir and Yarligan [31]. Maye and Venanzi have calculated rotational barrier and energies of both T_2 and T_1 tautomeric forms of 4-PI [32]. They reported that the difference in energy is 7.5 kJ/mol by T_2 compared with T_1. In the present work it is clear that the T_2 tautomer has the lowest energy and is the most stable form. The energy difference between T_1 and T_2 tautomer is 6.70 kJ/mol (at B3LYP/6-311G++(*d*,*p*) level of theory). This confirms that the 4-ClPI is the only stable tautomer in gas phase. The chloride atom is connected to para position in 4-phenylimidazole and 4-ClPI have similar tautomeric forms. The tautomeric equilibrium structures of phenylimidazole molecule were investigated in our previous paper [19] and is determined that T_2 is more stable than T_1 by 5.27 kJ/mol for B3LYP/6-311G(*d*,*p*) level of theory. So finally we taken tautomeric form was used in the future-calculations such as vibrational and NMR spectra of the 4-ClPI molecule.

Conformation Analysis

In order to reveal all possible conformations of 4-ClPI a detailed potential energy surface (PES) scan in N_{13}–C_{11}–C_3–C_2 dihedral angles was performed. The scan was carried out by minimizing the potential energy in all geometrical parameters by changing the torsion angle for every 10° for a 180° rotation around the bond. The shape of the potential energy as a function of the dihedral angle is illustrated in Fig. 4. It shows that T_2 tautomeric form was planar (N–C–C–C dihedral angle for 0°) and T_1 tautomeric form was twisted (N–C–C–C dihedral angle for 30°).

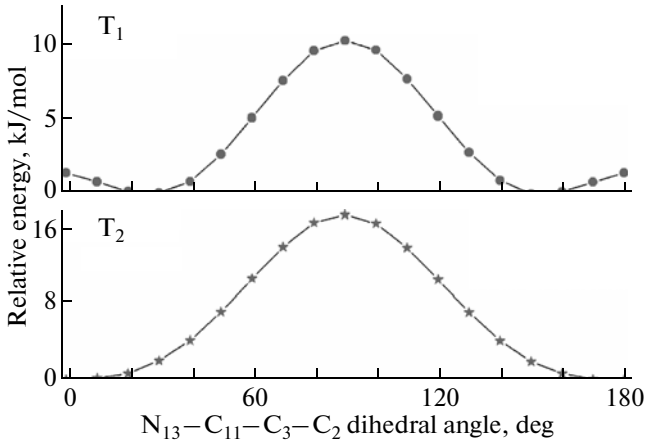

Fig. 4. Potential energy surface of tautomeric forms for $N_{13}-C_{11}-C_3-C_2$ dihedral angle.

Optimized Structure

The optimized bond lengths and bond angles of the T_2 tautomeric, form of the 4-ClPI molecule at B3LYP/6-311++G(*d*,*p*) level is collected in Table 1. These optimized geometric parameters of 4-PI are compared with those of X-ray data [33].

VIBRATIONAL ANALYSIS

The 4-ClPI molecule consists of 19 atoms. So there are 51 vibrational modes. The 51 vibrational modes of 4-ClPI have been assigned according to the detailed motion of the individual atoms. This molecule belongs to C_1 symmetry group. The experimental FT-IR and FT-Raman along with the calculated wavenumbers are given in Table 2. As seen in table, IR and Raman intensities of 4-ClPI are in consistency with the TED results.

The theoretically predicted IR and Raman spectra at B3LYP/6-311++G(*d*,*p*) level of calculations along with experimental FT-IR and FT-Raman spectra are shown in Figs. 1, 2.

The C–H stretching vibrations give rise to bands in the region 3100–3000 cm^{-1} in all the aromatic compounds [34–36]. The 4-ClPI molecule gives rise to six C–H stretching vibrations. The C–H stretching vibrations of imidazole group give rise to higher wavenumbers than those of phenyl group. Four of them belong to imidazole group. 3133 cm^{-1} (FT-IR spectra) and 3152 cm^{-1} (FT-Raman spectra) peak assigned to the CH stretching vibration of imidazole group. This peak is predicted at 3164 cm^{-1} by B3LYP/6-311++G(*d*,*p*) level of theory The C–H stretching vibrational bands of phenyl group are observed at 3065 cm^{-1} (3071 cm^{-1} for FT-Raman spectra and 3068 cm^{-1} for DFT calculation), 3113 cm^{-1} (3120 cm^{-1} for FT-Raman spectra and 3137 cm^{-1} for DFT calculation) in the FT-IR spectra. All the C–H stretching vibrations are within the expected range.

The C–H in-plane bending vibrations appears in the region 1300–1000 cm^{-1}. Peaks 1091, 1177, 1214, and 1284 cm^{-1} are assigned to C–H in-plane bending vibrations in the FT-IR spectra. The corresponding peaks are observed at 1096, 1157, 1183, and 1292 cm^{-1} in the FT-Raman spectra. The computations predict the bands at 1096, 1162, 1194, and 1290 cm^{-1}, respectively. The C–H out-of-plane bending vibrations occur in the range 1000–750 cm^{-1} for substituted benzenes [37]. In our title molecule weak to medium bands observed in FT-R as well as in FT-Raman spectrum at 730 cm^{-1} (mode no. 18), 774 cm^{-1} (mode no. 19), 832 cm^{-1} (mode no. 21) and 951 cm^{-1} (mode no. 25) and 777 cm^{-1} (mode no. 19), 812 cm^{-1} (mode no. 20), 843 cm^{-1} (mode no. 21), and 954 cm^{-1} (mode no. 25) are assigned to C–H in-plane bending vibrations for aromatic ring show good agreement with computed wavenumbers by B3LYP/6-311++G(*d*,*p*) method.

The heteroaromatic molecule containing an N–H group and its stretching absorption occur in the region 3500–3220 cm^{-1}. The position of absorption in this region depends upon the degree of hydrogen bonding, and hence upon the physical state of the sample or the polarity of the solvent [19]. Primary amines examined in dilute solution display two weak absorption bands, one near 3500 cm^{-1} and the other near 3400 cm^{-1}. These bands represent, respectively, the asymmetric and symmetric N–H stretching modes [38]. The N–H stretching band of benzimidazole and 2-methylbenzimidazole were observed in the region 3460–3450 cm^{-1} [39]. In the present work, the theoretical calculation indicates the scaled frequency value at 3488 cm^{-1} (mode no. 51) is assigned to N–H stretching vibrations. The TED corresponds to this vibration is a pure mode with contribution of 100%, but the recorded spectra fails to show such kind of band in the above said region. The presence of N–H out-of-plane bending vibration in free behzimidazole was observed at 433 and 421 cm^{-1} for 2-methylbenzimidazole [39]. In the present work the band observed in FT-IR spectrum at 450 cm^{-1} (463 cm^{-1} for FT-Raman spectra and 491 cm^{-1} for DFT calculation) and 509 cm^{-1} (529 cm^{-1} for FT-Raman spectra and 501 cm^{-1} for DFT calculation) are assigned to N–H out-of-plane bending vibrations. The N–H in-plane bending vibration computed by B3LYP/6-311++G(*d*,*p*) method show good agreement with recorded spectral data.

The identification of wavenumber for C–N stretching in the side chains is rather difficult since there are problems in differentiating those wavenumber from others. James et al. [40] assigned 1370 cm^{-1} for 1-benzyl-1-H-imidazole for C–N vibration. Pinchas et al. [41] assigned the C–N stretching at

Table 1. Optimized geometric parameters of 4-ClPI

Bond lengths, Å			Bond angles, deg			Dihedral angles, deg		
Parameters	B3LYP	X-Ray*	Parameters	B3LYP	X-Ray*	Parameters	B3LYP	X-Ray*
$C_1–C_2$	1.391	1.378	$C_2–C_1–C_6$	119.3	119.9	$C_6–C_1–C_2–C_3$	0.0007	0.600
$C_1–C_6$	1.390	1.388	$C_2–C_1–H_7$	120.5	115.1	$C_6–C_1–C_2–H_8$	179.9	179.4
$C_1–H_7$	1.082	0.992	$C_6–C_1–H_7$	120.0	124.8	$H_7–C_1–C_2–C_3$	−179.9	−176.5
$C_2–C_3$	1.401	1.385	$C_1–C_2–C_3$	121.1	121.2	$H_7–C_1–C_2–H_8$	−0.0007	2.310
$C_2–H_8$	1.082	0.956	$C_1–C_2–H_8$	120.0	118.2	$C_2–C_1–C_6–C_5$	−0.002	0.100
$C_3–C_4$	1.402	1.394	$C_3–C_2–H_8$	118.7	120.5	$C_2–C_1–C_6–Cl_{18}$	179.9	–
$C_3–C_{11}$	1.468	1.470	$C_2–C_3–C_4$	118.1	118.4	$H_7–C_1–C_6–C_5$	179.9	177.0
$C_4–C_5$	1.390	1.388	$C_2–C_3–C_{11}$	119.9	121.5	$H_7–C_1–C_6–Cl_{18}$	−0.002	–
$C_4–H_9$	1.084	0.965	$C_4–C_3–C_{11}$	121.8	120.0	$C_1–C_2–C_3–C_4$	0.002	−1.340
$C_5–C_6$	1.391	1.367	$C_3–C_4–C_5$	121.2	119.9	$C_1–C_2–C_3–C_{11}$	−179.9	−178.5
$C_5–H_{10}$	1.082	1.017	$C_3–C_4–H_9$	120.2	118.3	$H_8–C_2–C_3–C_4$	−179.9	−179.8
$C_6–Cl_{18}$	1.760	–	$C_5–C_4–H_9$	118.4	121.0	$H_8–C_2–C_3–C_{11}$	0.005	−2.280
$C_{11}–C_{12}$	1.379	1.373	$C_4–C_5–C_6$	119.1	121.0	$C_2–C_3–C_4–C_5$	−0.002	1.380
$C_{11}–N_{13}$	1.383	1.384	$C_4–C_5–H_{10}$	120.6	120.3	$C_2–C_3–C_4–H_9$	179.9	172.7
$C_{12}–H_{14}$	1.076	0.947	$C_6–C_5–H_{10}$	120.1	118.5	$C_{11}–C_3–C_4–C_5$	179.9	176.5
$C_{12}–N_{17}$	1.377	1.370	$C_1–C_6–C_5$	120.8	119.3	$C_{11}–C_3–C_4–H_9$	−0.010	−5.220
$N_{13}–C_{15}$	1.309	1.306	$C_1–C_6–Cl_{18}$	119.6	–	$C_2–C_3–C_{11}–C_{12}$	179.9	137.4
$C_{15}–H_{16}$	1.079	0.793	$C_5–C_6–Cl_{18}$	119.4	–	$C_2–C_3–C_{11}–N_{13}$	0.002	38.49
$C_{15}–N_{17}$	1.365	1.336	$C_3–C_{11}–C_{12}$	129.1	127.9	$C_4–C_3–C_{11}–C_{12}$	−0.027	40.44
$N_{17}–H_{19}$	1.007	1.069	$C_3–C_{11}–N_{13}$	121.4	122.9	$C_4–C_3–C_{11}–N_{13}$	180.0	143.6
			$C_{12}–C_{11}–N_{13}$	109.4	108.9	$C_3–C_4–C_5–C_6$	0.0004	−0.720
			$C_{11}–C_{12}–H_{14}$	132.6	137.9	$C_3–C_4–C_5–H_{10}$	−180.0	−178.7
			$C_{11}–C_{12}–N_{17}$	105.6	106.7	$H_9–C_4–C_5–C_6$	−179.9	−171.8
			$H_{14}–C_{12}–N_{17}$	121.6	116.0	$H_9–C_4–C_5–H_{10}$	0.004	7.630
			$C_{11}–N_{13}–C_{15}$	106.2	104.4	$C_4–C_5–C_6–C_1$	0.002	−0.040
			$N_{13}–C_{15}–H_{16}$	126.0	126.8	$C_4–C_5–C_6–Cl_{18}$	−179.9	–
			$N_{13}–C_{15}–N_{17}$	111.4	114.1	$H_{10}–C_5–C_6–C_1$	−179.9	−179.2
			$H_{16}–C_{15}–N_{17}$	122.5	118.5	$H_{10}–C_5–C_6–Cl_{18}$	0.002	–
			$C_{12}–N_{17}–C_{15}$	107.2	105.6	$C_3–C_{11}–C_{12}–H_{14}$	0.008	−8.870
			$C_{12}–N_{17}–H_{19}$	126.1	125.4	$C_3–C_{11}–C_{12}–N_{17}$	179.9	176.2
			$C_{15}–N_{17}–H_{19}$	126.5	128.7	$N_{13}–C_{11}–C_{12}–H_{14}$	−180.0	−174.7
						$N_{13}–C_{11}–C_{12}–N_{17}$	−0.034	−0.130
						$C_3–C_{11}–N_{13}–C_{15}$	−179.9	−176.7
						$C_{12}–C_{11}–N_{13}–C_{15}$	0.034	−0.110
						$C_{11}–C_{12}–N_{17}–C_{15}$	0.021	0.310
						$C_{11}–C_{12}–N_{17}–H_{19}$	180.0	175.8
						$H_{14}–C_{12}–N_{17}–C_{15}$	180.0	175.8
						$H_{14}–C_{12}–N_{17}–H_{19}$	−0.001	8.230
						$C_{11}–N_{13}–C_{15}–H_{16}$	179.9	172.1
						$C_{11}–N_{13}–C_{15}–N_{17}$	−0.020	0.320
						$N_{13}–C_{15}–N_{17}–C_{12}$	−0.001	−0.410
						$N_{13}–C_{15}–N_{17}–H_{19}$	−179.9	−175.3
						$H_{16}–C_{15}–N_{17}–C_{12}$	−180.0	−172.9
						$H_{16}–C_{15}–N_{17}–H_{19}$	0.002	2.800

*[33]

Table 2. Comparison of calculated and experimental (FT-IR and FT-Raman) vibrational spectra and related assignments of 4-ClPI

Mode no.	Frequency	I^b_{IR}	I^c_{Raman}	Exp. IR	Exp. Raman	TED, %
ν_1	30	3.770	0.777			$T_{CCCC}(52) + T_{CCCN}(46)$ I–P
ν_2	66	0.769	0.361		92	$T_{ClCCC}(16) + T_{CCCH}(10) + T_{CCCC}(32)$ P + $T_{NCCC}(13)$
ν_3	123	2.506	0.439		114	$\delta_{CCC}(65) + \delta_{CCN}(15) + \delta_{ClCC}(11)$ I–P
ν_4	187	5.377	0.567		142	$T_{NCCC}(20) + T_{CNCC}(13) + T_{ClCCC}(25) + T_{ClCCH}(13)$
ν_5	273	0.583	9.827		237	$\nu_{ClC}(36) + \delta_{CCC}(18)$ P
ν_6	283	2.631	0.281			$\delta_{ClCC}(71)$ P
ν_7	337	3.668	3.129		315	$T_{CCCC}(26) + T_{NCCC}(10) + T_{ClCCC}(18) + T_{ClCCH}(11)$P
ν_8	402	0.058	0.001		401	$T_{CCCC}(67) + \gamma_{CCH}(22)$ P
ν_9	445	2.911	2.210	418	419	$\delta_{CCC}(52) + \delta_{NCC}(18) + \delta_{ClCC}(10)$ I–P
ν_{10}	491	100	0.381	450	463	$\gamma_{CNH}(14) + \gamma_{NCH}(38)$ I
ν_{11}	493	23.45	2.301			$\nu_{ClC}(45) + \nu_{CC}(19)$ P
ν_{12}	501	0.339	0.838	509	529	$T_{CCCC}(20) + \gamma_{CCH}(36)$ P
ν_{13}	624	1.492	0.264	622	632	$T_{CNCC}(23) + \gamma_{NCH}(18) + \gamma_{CNH}(19)$ I
ν_{14}	624	0.410	3.897			$\delta_{CCC}(55) + \delta_{CCH}(18)$ P
ν_{15}	676	0.070	0.021	669		$\gamma_{NCH}(18) + T_{CNCC}(11) + T_{NCNC}(12)$ I
ν_{16}	697	2.029	0.119	684	694	$T_{CCCC}(38) + \gamma_{CCH}(17)$ P
ν_{17}	720	6.774	5.732	715	721	$\nu_{CC}(18) + \nu_{ClC}(25) + \delta_{CCC}(21)$ P
ν_{18}	740	21.94	1.058	730		$\gamma_{CCH}(41) + \gamma_{NCH}(12)$ I–P
ν_{19}	792	37.21	0.616	774	777	$\gamma_{CCH}(58) + \gamma_{NCH}(27)$ I
ν_{20}	800	5.751	0.168		812	$\gamma_{CCH}(86)$ P
ν_{21}	826	26.07	0.462	832	843	$\gamma_{CCH}(44) + \gamma_{ClCH}(30)$
ν_{22}	910	19.85	8.716	908	891	$\nu_{CC}(10)$P + $\delta_{CCN}(23) + \delta_{CNC}(20)$ I
ν_{23}	920	3.178	1.423		926	$\delta_{CNC}(30) + \delta_{CCN}(11) + \delta_{NCN}(16)$ I
ν_{24}	923	0.000	0.084			$\gamma_{CCH}(74)$ P
ν_{25}	956	0.300	0.070	951	954	$\gamma_{CCH}(89)$ P
ν_{26}	994	19.51	3.935	1007	995	$\nu_{CC}(16) + \delta_{CCC}(41) + \delta_{CCH}(26)$ P
ν_{27}	1039	12.36	4.632		1015	$\nu_{CC}(25)$ P + $\nu_{NC}(17) + \delta_{NCH}(23)$ I
ν_{28}	1063	20.40	13.90	1061	1064	$\nu_{CC}(52) + \nu_{ClC}(16)$ P
ν_{29}	1076	50.76	1.133			$\nu_{CC}(25) + \delta_{CCH}(30) + \delta_{CNH}(15)$ I
ν_{30}	1089	11.88	4.996			$\nu_{CC}(22) + \delta_{CNH}(35)$ I
ν_{31}	1096	22.33	2.342	1091	1096	$\nu_{CC}(17) + \nu_{NC}(24) + \delta_{CCH}(33)$ I–P
ν_{32}	1162	0.407	8.938	1177	1157	$\nu_{CC}(17) + \delta_{CCH}(75)$ P
ν_{33}	1194	3.354	2.157	1214	1183	$\delta_{CCH}(45) + \delta_{NCH}(21)$ I
ν_{34}	1255	6.574	9.811	1246	1248	$\nu_{CC}(37) + \nu_{NC}(23) + \delta_{NCH}(10)$ I–P
ν_{35}	1273	4.013	3.854		1277	$\nu_{CC}(66) + \delta_{CCH}(12)$ P
ν_{36}	1290	3.045	10.27	1284	1292	$\nu_{CC}(17) + \delta_{CCH}(57)$ P
ν_{37}	1309	0.993	15.89	1312	1312	$\nu_{CC}(13) + \nu_{NC}(50) + \delta_{NCH}(18)$ I
ν_{38}	1385	4.067	3.487			$\nu_{CC}(36) + \delta_{CCH}(35)$ P
ν_{39}	1401	19.35	34.65	1400	1403	$\nu_{CC}(38) + \delta_{CNH}(39)$ I
ν_{40}	1458	33.51	3.731	1453	1466	$\nu_{CC}(46) + \delta_{CCH}(23)$ P
ν_{41}	1480	64.24	3.556	1483	1489	$\nu_{CN}(35) + \delta_{NCH}(12) + \delta_{CNH}(12)$ I
ν_{42}	1528	5.826	48.08	1505	1515	$\nu_{CC}(45) + \delta_{CCH}(11)$ I–P
ν_{43}	1557	0.241	5.783	1576	1565	$\nu_{CC}(67)$ P
ν_{44}	1584	0.349	100	1603	1608	$\nu_{CC}(66) + \delta_{CCH}(11)$ P
ν_{45}	3068	8.785	1.133	3065	3071	$\nu_{CH}(100)$ P
ν_{46}	3087	1.370	1.947			$\nu_{CH}(100)$ P
ν_{47}	3094	3.673	2.986			$\nu_{CH}(98)$ P
ν_{48}	3101	1.101	3.897	3113	3120	$\nu_{CH}(99)$ P
ν_{49}	3137	1.888	4.287			$\nu_{CH}(99)$ I
ν_{50}	3164	0.769	1.984	3133	3152	$\nu_{CH}(99)$ I
ν_{51}	3488	82.33	4.750			$\nu_{NH}(100)$ I

Note: Obtained from the wave numbers calculated at B3LYP/6-311++G(*d*,*p*) using scaling factors 0.967 (for wave numbers under 1800 cm^{-1}) and 0.955 (for those over 1800 cm^{-1}). Relative absorption intensities normalized with highest peak absorption equal to 100. Relative Raman intensities calculated by Raint software and normalized to 100. Total energy distribution (TED) calculated B3LYP/6-311++G(*d*,*p*) level, TED less than 10% are not shown.

1368 cm^{-1} in benzamide. Kahovec and Kohlreusch [42] identified the stretching wavenumber of C=N band in salicylicaldoxinne at 1617 cm^{-1}. In the present work 1480 and 1309 cm^{-1} in the FT-IR spectra peaks are assigned to the CN stretching vibrations. The CN stretching, vibrations are observed at 1489 and 1316 cm^{-1} in the FT-Raman spectra, respectively. The CC stretching mode occurs at lower wavenumbers than CH stretching vibrations of the aromatic ring. Aromatic C=C stretching vibrations occur in the region 1625–1430 cm^{-1} IR [43]. C–C stretching bands are observed at 1603 cm^{-1} (1584 cm^{-1} for DFT and 1608 cm^{-1} for FT-Raman), 1576 cm^{-1} (1577 cm^{-1} for DFT and 1565 cm^{-1} for FT-Raman), 1505 cm^{-1} (1528 cm^{-1} for DFT and 1515 cm^{-1} for FT-Raman), 1453 cm^{-1} (1458 cm^{-1} for DFT and 1466 cm^{-1} for FT-Raman), 1400 cm^{-1} (1401 cm^{-1} for DFT and 1403 cm^{-1} for FT-Raman), and 1246 cm^{-1} (1255 cm^{-1} for DFT and 1248 cm^{-1} for FT-Raman). Peak 1277 cm^{-1} (1273 cm^{-1} for DFT) is assigned to the CC stretching vibration in the FT-Raman spectra and is not observed in the FT-IR spectra.

For simple organic chlorine compounds C–Cl absorptions are in the region 1129–480 cm^{-1}[44, 45]. In the FT-IR spectrum of 4-ClPI 715 cm^{-1} and 1061 cm^{-1} is assigned to C–Cl stretching vibration. These vibrations are observed at 721 and 1064 cm^{-1}, respectively. The theoretical calculation by DFT method at 493, 720, and 1063 cm^{-1} exactly correlates with experimental observation. Peak 493 cm^{-1} is not experimentally observed in the FT-IR and FT-Raman spectra. The C–Cl in-plane and out-of-plane bending vibrations are predicted at 283 cm^{-1} (mode no. 6) and 66 cm^{-1} (mode no. 2), respectively. Out-of-plane vibration is observed at 92 cm^{-1} in the FT-Raman spectra. But in-plane vibration is not observed in the FT-Raman spectra. These observations are supported by the literature [46, 47]. According to the literature, all the C–Cl vibrations are in the predictable range.

NMR ANALYSIS

The isotropic chemical shifts are frequently used as an aid in identification of organic compounds and accurate predictions of molecular geometries are essential for reliable studies of magnetic properties. The B3LYP method allows calculating the shielding constants with accuracy and the GIAO method is one of the most common approaches for calculating nuclear magnetic shielding tensors. The ^1H and ^{13}C NMR isotropic shielding were calculated using the GIAO method [24, 26] using the optimized parameters obtained from B3LYR/6-311++G(*d*,*p*) method. The effect of solvent on the theoretical NMR parameters was included using the default model IEF-PCM provided by Gaussian 09. The isotropic shielding values were used to calculate the isotropic chemical shifts

Table 3. The experimental and predicted ^{13}C and ^1H isotropic chemical shifts (with respect to TMS, all values in ppm) for 4-ClPI

Atom	Experiment	B3LYP	Atom	Experiment	B3LYP
C_{11}	150.08	145.432	H_{19}	8.20	8.916
C_6	143.69	144.543	H_8	7.64	8.435
C_{15}	134.97	139.258	H_9	7.64	7.841
C_3	134.40	139.205	H_{14}	7.60	7.790
C_1	129.00	133.358	H_{16}	7.33	7.609
C_5	129.00	133.273	H_{10}	7.22	7.414
C_2	128.96	129.948	H_7	7.22	7.408
C_4	128.96	128.909			
C_{12}	120.06	118.013			

δ with respect to tetramethylsilane (TMS): $\delta_{iso}(X) = \sigma_{TMS}(X) - \sigma_{iso}(X)$, where δ_{iso}—isotropic chemical shift and σ_{iso}—isotropic shielding.

As in Fig. 3 the studied molecule shows seven different carbon atoms. Taking, into account that the range of ^{13}C NMR chemical shift for analogous organic molecules, usually is more 100 ppm [48, 49], the accuracy ensures reliable interpretation of spectroscopic parameters. In the present work ^{13}C NMR chemical shifts in the ring for the title molecule are more 100 ppm as they would be expected (Table 3).

The linear correlations between calculated and experimental data of ^{13}C NMR and ^1H NMR spectra are noted. Correlation coefficients of ^{13}C NMR and ^1H NMR are determined as 0.864 and 0.877 for

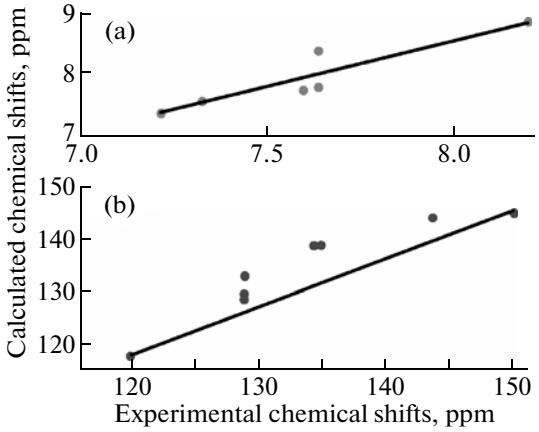

Fig. 5. The relationship between the experimental chemical shift and computed GIAO/B3LYP/6-311++G(*d*,*p*) levels for ^1H (a) and ^{13}C (b).

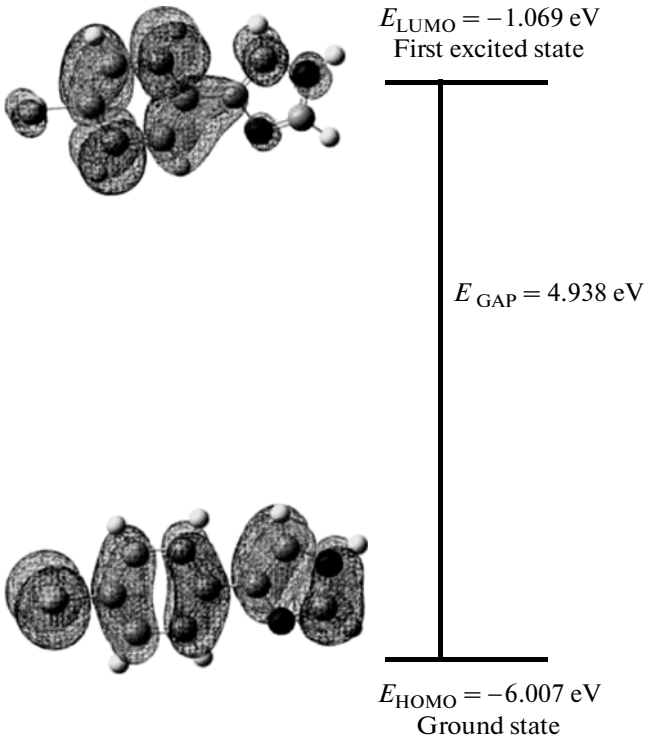

Fig. 6. The frontier molecular orbitals of 4-ClPI.

4-ClPI. The data shows a good correlation between predicted and observed proton and carbon chemical shifts. The correlations of NMR spectra are presented in Fig. 5 for 4-ClPI.

HOMO-LUMO ANALYSIS

The atomic orbital compositions of the frontier molecular orbitals of 4-ClPI is shown in Fig. 6. The HOMO-LUMO energy gap of these compounds was calculated at the B3LYP/6-311++G(*d*,*p*) level. The HOMO represents the ability to donate an electron, LUMO as an electron acceptor represents the ability to obtain an electron. Both HOMO and LUMO are the main orbitals that take part in chemical stability. The eigenvalues of LUMO and HOMO and their energy gap reflect the chemical activity of the molecule.

The decrease in the HOMO and LUMO energy gap explains the eventual charge transfer interaction taking place within the molecule which is responsible for the activity of the molecule. Consequently, the lowering of the HOMQ-LUMO band gap is essentially a consequence of the large stabilization of the LUMO due to the strong electron-acceptor ability of the electron-acceptor group.

MULLIKEN CHARGE DISTRIBUTION ANALYSIS

As seen in Table 4 the Mulliken atomic charges were calculated at the B3LYP/6-311++G(*d*,*p*) basis set. Figure 7 shows the Mulliken atomic net charges in 4-ClPI. Nature of C atom have negative charge but in 4-ClPI except C_3, C_6, C_{12}, and C_{15} having positive (0.6645, 0.4203, 0.1279, and 0.2742e) charge, showing that these are bonded with heavy electronegative atoms (C-imidazole ring, C–Cl, C–N). Normally hydrogen atoms have positive charge, but in 4-ClPI H_{19} having more positive charge(0.3324e) in comparision with other hydrogen atoms, it shows that the electron pass through into the nitrogen atom to the imidazole ring. The atoms N_{17} (–0.1883e) is more negative charge than N_{13} (–0.0996e).

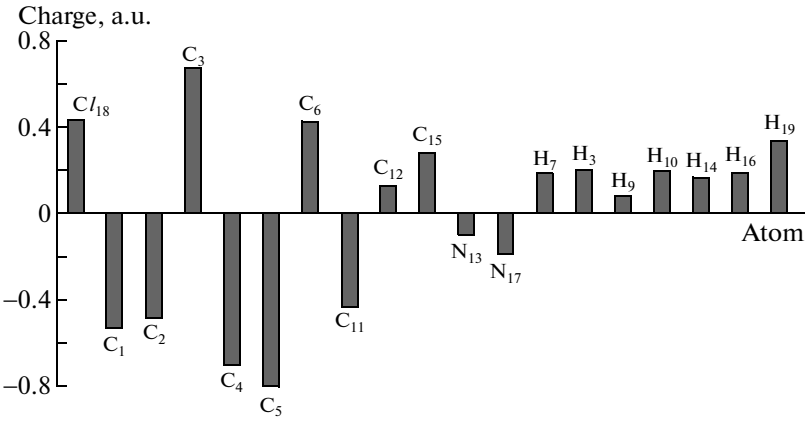

Fig. 7. Mulliken atomic charge of 4-ClPI.

Table 4. Mulliken atomic charge of 4-ClPI

Atom	Charge
Cl_{18}	0.4292
C_1	−0.5337
C_2	−0.4845
C_3	0.6645
C_4	−0.7000
C_5	−0.8008
C_6	0.4203
C_{11}	−0.4319
C_{12}	0.1279
C_{15}	0.2742
N_{13}	−0.0996
N_{17}	−0.1883
H_7	0.1812
H_8	0.1994
H_9	0.0781
H_{10}	0.1888
H_{14}	0.1574
H_{16}	0.1853
H_{19}	0.3324

CONCLUSION

The optimized molecular structures, NMR spectra, vibrational frequencies and corresponding vibrational assignments of 4-ClPI have been calculated using B3LYP/6-311++G(*d*,*p*) method. Comparison of the experimental and calculated spectra of the molecule showed that DFT-B3LYP method is in good agreement with experimental data. On the basis of agreement between the calculated and observed results, assignments of fundamental vibrational modes of 4-ClPI were examined and some assignments were proposed. This study demonstrates that scaled DFT/B3LYP calculations are powerful approach for understanding the vibrational spectra of medium sized organic compounds. ^1H and ^{13}C NMR chemical shifts have been compared with experimental values.

ACKNOWLEDGMENTS

This work was supported by the Research Fund of Ahi Evran University, Project Number: FBA-11009.

REFERENCES

1. C. F. Claiborne, N. J. Liverton, and K. T. Nguyen, Tetrahedron Lett. **39**, 8939 (1998).
2. Q. Ahao, S. J. Liu, M. Shi, F. Y. Li, H. Jinh, and T. Yi, Organometall. **26**, 5922 (2007).
3. A. Pesquet, A. Daiech, and H. L. Van, J. Org. Chem. **71**, 5303 (2006).
4. F. Bellina, S. Cauteruccio, S. Montib and R. Rossi, Biorg. Med. Chem. Lett. **16**, 5757 (2006).
5. W. Peter and K. Wilhelm, Ang. Chem. **39**, 3772 (2000).
6. F. Bellina, S. Cauteruccio, and R. Rossi, Tetrahedron **63**, 4571 (2007).
7. S. Pakr, O. H. Kwon, S. Kim, S. Park, M. G. Choi, and M. Cha, J. Am. Chem. Soc. **127**, 100070 (2005).
8. Y. F. Sun and Y. P. Cui, Dyes and Pigm. **81**, 27 (2009).
9. U. Ucucu, N. G. Karaburun, and I. Isikdag. Farmaco **56**, 285 (2001).
10. T. Kamidate, K. Yamaguchi, T. Segawa, and H. Watanabe, Loph. Anal. Sci. **5**, 429 (1989).
11. L. Zhao, S. B. Li, G. A. Wen, B. Peng, and W. Yuang, Mater. Chem. Phys. **100**, 460 (2006).
12. G. Zhang, H. Guo, Y. Chuai, and D. Zou, Mater. Lett. **59**, 2003 (2005).
13. Q. F. Xiang, R. G. Evans, M. J. Edirisinghe, and P. F. Blazdell, Proc. Inst. Eng. B **211**, 211 (1997).
14. C. Louis, R. Bazzi, C. A. Marquette, J. L. Bridot, S. Roux, G. Ledoux, B. Mercier, L. Blum, P. Perriat, and O. Tillement, Chem. Mater. **17**, 1673 (2005).
15. W. A. Adams, M. G. Bakker, and T. I. Quickenden, Photochem. Photobiol. A **181**, 166 (2006).
16. C. C. Lee, J. C. Wnag, and A. T. Hu, Mater. Lett. **58**, 535 (2004).
17. E. Gondek, I. V. Kityk, A. Danel, A. Wisa, and J. Sanetra, Synthetic Metals **156**, 1348 (2006).
18. E. Gondek, I. V. Kityk, J. Sanetra, P. Szlachcic, P. Armatys, A. Wisla, and A. Danel. Opt. Las. Technol. **38**, 487 (2006).
19. M. T. Gulluoglu, Y. Erdogdu, J. Karpagam, N. Sundaraganesan, and S. Yurdakul, J. Mol. Struct. **990**, 14 (2011).
20. M. J. Frisch et al., Gaussian 09. Revision A. 02 (Gauss. Inc. Wallingford CT, 2009).
21. G. Rauhut and P. Pulay, J. Phys. Chem. **99**, 3093 (1995).
22. Y. Erdogdu, O. Unsalan, and M. T. Güllüoğlu, J. Raman Spectrosc. **41**, 820 (2010).
23. Y. Erdogdu, O. Unsalan, M. Amalanathan, and J. I. Hubert, J. Mol. Struct. **980**, 24 (2010).
24. Y. Erdogdu, O. Ünsalan, D. Sajan, and M. T. Güllüoğlu, Spectrochim. Acta A **76**, 130 (2010).
25. R. Ditchfield, **56**, 5688 (1972).
26. K. Wolinski, J. F. Hinton, and P. Pulay, J. Amer. Chem. Soc. **112**, 8251 (1990).
27. N. Azizi, A. A. Rostami, and A. Godarzian, J. Phys. Soc. Japan **74**, 1609 (2005).
28. M. Rohlfing, C. Leland, C. Allen, and R. Ditchfield, Chem. Phys. **87**, 9 (1984).
29. D. Michalska, Raint Program, Wroclaw University of Technology, 2003.
30. D. Michalska and R. Wysokinski, Chem. Phys. Lett. **403**, 211 (2005).
31. C. Ogretir and S. Yarligan, J. Mol. Struct. **425**, 249 (1998).
32. P. V. Maye and C. A. Venanzi, Struct. Chem. **1**, 517 (1990).

33. R. M. Claramunt, M. D. S. Maria, L. Infantes, F. H. Cano, and J. Elguero, J. Chem. Soc. Perkin Transact. **2**, 564 (2002).

34. G. Socrates, *Infrared Characteristic Group Frequencies* (Wiley, New York, 1980).

35. G. Varsanyi, *Vibrational Spectra of Benzene Derivatives* (Academic, New York, 1969).

36. M. Silverstein, G. C. Basseler, and C. Morill, *Spectrometric Identification of Organic Compounds* (Wiley, New York, 1981).

37. M. K. Subramanian, P. M. Andarasan, V. Ilangovan, and N. Sundaraganesan, Molec. Simul. **34**, 277 (2008).

38. S. Gunasekaran, R. Thilak Kumar, and S. Ponnusamy, Spectrochim. Acta A **65**, 1041 (2006).

39. R. I. Castillo, L. A. R. Montalvo, and S. P. H. Rivera, J. Mol. Struct. **877**, 10 (2007).

40. C. James, C. Ravikumar, V. S. Jayakumar, and J. Hubert, J. Raman Spectrosc. **40**, 537 (2009).

41. S. Pinchas, D. Samuel, and M. Weiss-Broday, J. Chem. Soc. **1**, 1688 (1961).

42. T. S. Xavier, N. Rashid, and Joe Huber, Spectrochim. Acta A **78**, 319 (2011).

43. G. Socrates, *Infrared and Raman Characteristic Group Frequencies* (Wiley, Chichester, 2001).

44. S. Ramalingam, P. Andusrinivasan, and S. Periandy, Spectrochim. Acta A **78**, 826 (2011).

45. K. Rastogi, M. A. Palafox, R. P. Tanwar, and L. Mittal, Spectrochim. Acta A **58**, 1989 (2002).

46. W. O. George, P. S. McIntyre, and D. J. Mowthorpe, *Infrared Spectrscopy* (Wiley, New York, 1987).

47. M. A. Palafox, V. K. Rastogi, and L. Mittal, Int. J. Quant. Chem. **94**, 189 (2003).

48. H. O. Kalinowski, S. Berger, and S. Braun, *C-13 NMR Spectroscopy* (Wiley, Chichester, 1988).

49. K. Pihlaja and E. Kleinpeter, *Carbon–13 Chemical Shifts in Structural and Stereo-Chemical Analysis* (VCH Publishers, Deerfield Beach, FL, 1994).